Polarized IR reflectance study of GaN thin films: The effects of incidence angles on the optical phonon modes

S. S. Ng, Z. Hassan and H. Abu Hassan

Nano-Optoelectronics Research and Technology Laboratory

School of Physics, Universiti Sains Malaysia, 11800 Penang, Malaysia

Tel.: 604-6533673

Fax: 604-6579150

ABSTRACT

In this work, we report on the effects of incidence angles on the IR optical phonon modes of GaN thin films grown on 6H-SiC substrate. Room temperature polarized IR reflectance measurements were carried out using Fourier transform infrared (FTIR) spectroscopy at various incidence angles, namely, from 15° – 75°. The reflection spectra are compared to the calculated spectra generated with a damped single harmonic oscillator model. Good agreement between the measured and calculated spectra has been obtained. Through this model fit, complete sets of reststrahlen parameters unambiguously assigned to GaN thin films and 6H-SiC substrate were obtained. It was found that the changes of the reststrahlen bands shape as a function of the incidence angle is more significant for the p-polarized spectra than the s-polarized spectra. As the angle of incidence was increased, the s-polarized spectra retain their overall shape; while the p-polarized spectra become distorted especially near to the LO phonon modes of the GaN thin films where the reststrahlen band shapes are distorted and a new feature was slowly formed, the LO phonon modes of the GaN

thin films however remain unchanged. Overall, we have found that the optical phonon modes are independent of the angle of the incidence beam.

Keywords: Gallium nitride; Fourier transform infrared spectroscopy; polarized infrared reflectance; reststrahlen band; Optical phonon modes;

I. INTRODUCTION

During the past few years, much attention have been paid to group-III nitride semiconductors especially gallium nitride (GaN) and its related compounds. This is because these materials are very promising particularly for optoelectronic applications operating in the blue and ultra-violet (UV) spectral range [1-3]. As a result, extensive research both in academic and in technological development has been carried out.

To date, a number of studies on the optical properties of the GaN in the IR region have been carried out by measuring the reflectivity of the thin films for IR radiation at normal or oblique incidence [4-16]. Additionally, more informative investigations on the GaN have also been conducted by means of polarized IR reflectance technique [17-24]. In spite of huge efforts, little is known about the effects of incidence angles on the optical phonon modes of GaN thin films. Knowledge of the effects of the incidence angles on the optical phonon modes is crucial for understanding the behaviour of the photon-phonon coupling and hence crucial for the designing of the optoelectronic devices.

Note that similar measurements have been conducted by Yu *et al.* [24]. They have reported the polarized IR reflection of GaN epilayer grown on sapphire substrate at three incidence angles (18°, 45°, and 75°). Their studies were mainly focused on the model fit and more attention has been paid to the sapphire. In addition, the changes in the GaN reststrahlen

band as a function of the incidence angles are not clear as compared to our results. This is due to the GaN reststrahlen band was superimposed on the reststrahlen band of the sapphire substrate. Apart from that, several authors have reported variable angles infrared ellipsometry (IRE) studies on GaN [25-28]. However, the interpretations of the IRE data are different as compared to the conventional polarized IR reflectance data. For IRE, the measurements need to be carried out at various incidence angles in order to obtain ellipsometric angles ψ and differential phase change Δ. With these sets of parameters, thickness as well as refractive index of the film, then the spectrum of ψ can be simulated from the numerical calculation. Subsequently, the optical parameters of the films can be obtained from the best fit of the experimental and theoretical spectrum. Hence, the IRE does not measure the film directly and it is a complicated method to investigate the interactions between the IR and phonons. The polarized IR reflectance measurements are more direct, i.e. a set of reststrahlen parameters can be obtained from a single IR measurement. In addition, polarized IR measurements at various angles of incidence may provide various sets of lattice dynamics information. For this reason, the interpretations from IRE results will not be concerned in this paper.

In this paper, we report on the IR reflectance study of GaN thin films grown on 6H-SiC substrate measured with s- and p-polarization at different incidence angles. Through this study, the effects of incidence angles on the reststrahlen bands shapes and the optical phonon modes of the GaN/6H-SiC were investigated. However, more attention will focus on the GaN thin films.

II. EXPERIMENTAL

In this work, the GaN epilayer sample with wurtzite structure was unintentionally doped n-type and was grown on 6H-SiC substrate. The carrier concentration of the GaN thin

film is about 3×10^{17} cm^{-3}. The GaN epilayer was grown with the crystallographic c axis along the growth direction and the thickness was ~ 0.33 μm. More details about the structural properties of this sample can be found elsewhere [29].

IR measurements were carried out by using a Fourier transform infrared (FTIR) spectrometer (Spectrum GX FT-IR, Perkin-Elmer) with a KBr beam splitter and a mid IR triglycine sulfate (TGS) detector. A wire grid zinc selenide (ZnSe) IR polarizer was used to obtain s- and p-polarization spectra, where the electric field vector ($\boldsymbol{E}$) is perpendicular ($\boldsymbol{E} \perp c$) and parallel ($\boldsymbol{E} \parallel c$) to the crystal axis respectively. All measurements were taken in the reflection mode at room temperature at a resolution of 1 cm^{-1} and the number of scans was 64. A Perkin-Elmer variable angle reflectance accessory (VASR) was used to measure the reflectance spectra at various incidence angles, namely, 15°, 30°, 45°, 60°, and 75°. An aluminium-coating mirror was employed as reference standards. The schematic diagram of the GaN/6H-SiC cross-section and the beam geometry of the polarization measurements is shown in Fig. 1.

III. THEORETICAL MODEL

Since, the GaN thin films used in this work have wurtzite structure with z oriented along the growth direction, c axis; hence, two sets of phonon parameters are required to describe the dielectric function, i.e. $\varepsilon_{xx} = \varepsilon_{yy} \equiv \varepsilon_{\perp}$ and $\varepsilon_{zz} \equiv \varepsilon_{\parallel}$ in the modes of $\boldsymbol{E} \perp c$ and $\boldsymbol{E} \parallel c$ to the crystal axis respectively [18]. For this reason, all measurements in this work were performed in the s- and p-polarization.

The Fresnel equations for the oblique incidence polarized IR reflectivity (R) are given by [18]:

$$R_{\perp} = \left[\frac{\cos\theta - \left(\varepsilon_{xx} - \sin^2\theta\right)^{1/2}}{\cos\theta + \left(\varepsilon_{xx} - \sin^2\theta\right)^{1/2}} \right]^2, \tag{1}$$

$$R_{\parallel} = \left\{ \frac{\cos\theta - \left[\frac{\left(\varepsilon_{zz} - \sin^2\theta\right)}{\varepsilon_{xx}\varepsilon_{zz}} \right]^{1/2}}{\cos\theta + \left[\frac{\left(\varepsilon_{zz} - \sin^2\theta\right)}{\varepsilon_{xx}\varepsilon_{zz}} \right]^{1/2}} \right\}^2, \tag{2}$$

where θ is the angle of incidence. From these equations, it can be seen that in s-polarization ($\boldsymbol{E} \perp c$) only ε_{xx} is sampled; whereas in p-polarization ($\boldsymbol{E} \parallel c$) both ε_{xx} and ε_{zz} are sampled, the relative proportions of the ε_{xx} and ε_{zz} being determined by the angle of incidence θ. Since the ε_{xx} and ε_{zz} are characterized by the $TO_{\perp}$ and $LO_{\parallel}$ [30] respectively, hence, the reflectance spectra for $\boldsymbol{E} \perp c$ and $E \parallel$ c are described by these optical phonon modes too. Consequently, only the $TO_{\perp}$ feature will appear in $\boldsymbol{E} \perp c$ spectrum, while both the $TO_{\perp}$ and $LO_{\parallel}$ features will turn up in $E \parallel$ c spectrum.

In this work, we have modelled the dielectric function ε ($\varepsilon_{\perp}$ and $\varepsilon_{\perp}$) for both the thin film and the substrate based on a damped single harmonic oscillator model [30]:

$$\varepsilon_{xx} = \varepsilon_{yy} = \varepsilon_{\perp} = \left(\varepsilon_{\infty} + \sum_j \frac{S_j w_{TOj}^2}{w_{TOj}^2 - w^2 - iw\,\gamma_j} \right)_{\perp}, \tag{3}$$

$$\varepsilon_{zz} = \varepsilon_{\parallel} = \left(\varepsilon_{\infty} + \sum_j \frac{S_j w_{TOj}^2}{w_{TOj}^2 - w^2 - iw\,\gamma_j} \right)_{\parallel}. \tag{4}$$

The subscript $\perp$ and $\|$ represents the modes of $\boldsymbol{E} \perp c$ and $\boldsymbol{E} \| c$ respectively. The ε_∞ is the high frequency dielectric constant. w_{TOj}, S_j and γ_j are, respectively, the transverse optical-phonon frequency, the phonon oscillator strength and the phonon damping of the j^{th} oscillator. The S is given by

$$S = \varepsilon_\infty \left(\frac{w_{LO}^2 - w_{TO}^2}{w_{TO}^2} \right). \tag{5}$$

In general, it represents the splitting of the transverse and longitudinal optical-phonon frequency (w_{TO} and w_{LO}) and hence described the width of the reststrahlen band.

In this work, the theoretical reflection spectra are generated by using Equations. (1) – (4). The values ε_∞ of both the GaN epilayer and the 6H-SiC substrate are obtained from Yu *et al.* [24] and Spitzer *et al.* [31] respectively. Through this model fit, a complete set of Brillouin zone (BZ) centre reststrahlen parameters unambiguously assigned to GaN thin films and 6H-SiC substrate can be obtained.

IV. RESULTS AND DISCUSSION

In general, the GaN reststrahlen region lies between 550 and 750 cm^{-1} whereas the 6H-SiC reststrahlen region lies between 750 and 1000 cm^{-1}. Consequently, both reststrahlen bands are well separated and the absorption due to the TO and the LO optical phonon modes both from the GaN thin films and from the 6H-SiC substrate can clearly be seen.

Fig. 2 shows the room temperature reflectance spectra of the GaN epilayer grown on 6H-SiC substrate measured with s- and p-polarization at various incidence angles. Overall, both sets of polarized spectra are similar, namely dominated by two high reflectivity features,

except that there are two pronounced dips in the p-polarized spectra. The two high reflectivity features centred at ~560 cm^{-1} and ~800 cm^{-1} correspond to the TO phonon modes of the GaN epilayer and 6H-SiC substrate respectively. Whereas, the two dips at ~732 cm^{-1} and ~974 cm^{-1} correspond to the LO phonon modes of the GaN epilayer and 6H-SiC substrate respectively; the presence of these dips can be attributed to the Berreman effects [32]. The feature centred at ~630 cm^{-1} in both spectra arises from the noise generated by aluminium coating mirror, which has been used during acquisition of the reference or background spectrum.

We consider now the effects of incidence angles on the reststrahlen bands and the optical phonon modes of the GaN/6H-SiC. For simplicity, we will describe the behaviour of the sample in each region separately. However, more attention will focus on the GaN thin films.

(a) GaN thin films

As mentioned previously, the reflection spectra are compared to the calculated spectra generated by using Equations (1) – (4). From Fig. 2, it can be seen that the fitting of theoretical spectra to the experimental spectra measured with s- and p-polarization at various incidence angles are good in each case. The parameters obtained from the best fit of our data are listed in Table I. It should be noted that the fitting uncertainty of the optical phonon modes frequencies (w_{TO} and w_{LO}) and the phonon damping (γ) for GaN epilayer (6H-SiC substrate) is ±0.5 (±1.0) and ±1.0 (±2.0) cm^{-1}, respectively. Overall, it can be seen that the values of the TO and LO phonon modes of GaN measured at s- and p-polarization are independent of the incidence angle. Although the shapes at the vicinity of the LO mode of GaN (in p-polarized spectra) changes with the angle of incidence, however, these effects does not influence the position of the TO and LO phonon modes of the GaN epilayer. This is also

evident from the equation (3) where the $\varepsilon_{\perp}$ (or $\varepsilon_{\parallel}$) is independent of the incidence angle θ. Detailed descriptions are given below.

For s-polarized spectra, it can be seen from the Fig. 2 and the Table I that no significant shift or distortion of both the shapes and the position of the reststrahlen band were detected as the angles of incidence increases. For p-polarized spectra, the changes of the reststrahlen band shapes as a function of the incidence angle is more significant than the s-polarization spectra. As shown in the p-polarized spectra, as the incidence angle increases, the feature due to the TO phonon mode remain the same while the feature due to the LO phonon mode become distorted. The reflectivity of the dip of the LO mode at first decreases (become deeper) then reaches a minimum value (at an incidence angle of 45°) and finally increases as the incidence angle increases. Furthermore, as the incidence angle increases, a new feature (or peak) near to the edge of the LO mode is slowly formed. Nevertheless, as evident from the model fit results, it is found that the position of the TO and LO phonon modes is unchanged. The distortion of the reststrahlen bands shape near to the LO phonon modes for the case of p-polarized is believed to be due to the change of the refractive index, n, and the extinction coefficient, k, in the vicinity of the LO mode, i.e. as a result of phase change after the Brewster angle [33]. In general, the phase change after the Brewster angle for s- and p-polarized measurements are zero and π respectively.

In this study, Kramers-Kronig dispersion relation has been used to obtain the n and k spectra. Fig. 3 shows the n and k, for s- and p-polarized measurements at various incidence angles. The inset figures in p-polarized spectra show the enlargement near the LO mode of GaN.

For s-polarized spectra, the shapes of the n and k spectra for 15° to 60° remain the same except at the incidence angle of 75° where the spectra at 75° are quite noisy at the lower wavenumber region. This is likely due to high intensities of the background noise (as can be

seen from the s-polarized reflectivity spectrum of 75° depicted in Fig. 2). Since the phase change between the incidence and the reflected s-polarized IR beam (before or after the Brewster angle) is always zero; hence, there are no distortions on the n and k as well as the reflectivity spectra. As a result, all the s-polarized spectra retain their shapes although the angle of incidence increased.

The situation is more complicated for the p-polarized measurements, because there was a phase shift between the incidence and the reflected polarized IR beam. Moreover, there was an abrupt change of π after the Brewster angle. Consequently, the changes of the reststrahlen bands shape as a function of the incidence angle is more significant than the s-polarized spectra.

For p-polarized spectra, as the θ changes from 15° to 60°, the distortions of the shapes of the n and k spectra is not that significant, except the shapes at the vicinity of the LO mode of GaN (see the enlargement in the p-polarized spectra of n and k). The shapes of the n and k spectra at the incidence angle of 75°, however, changes abruptly to derivative-like shapes due to the phase change of π after the Brewster angle, $\theta_B = \tan^{-1}(n_{\text{GaN}}/n_{\text{Air}}) \cong 66.5^\circ$ (by assuming the IR refractive indices $n_{\text{GaN}} = 2.3$ [34] and $n_{\text{air}} = 1$). It is important to note here that this θ_B equation is true by assuming no absorption. If the absorption occurs (i.e. the material has absorption bands at certain frequencies of light), the refractive index will become complex, $\tilde{n} = n + ik$. Consequently, the θ_B equation will become complex too [35]. Nevertheless, for the sake of simplicity, we still assume the $\theta_B \cong 66.5^\circ$.

In order to demonstrate the abrupt changes of the shapes of the n and k spectra at the θ_B, measurement at $\theta_B \cong 66.5^\circ$ with p-polarization has been carried out. The reflectivity spectrum and the corresponding spectra of n and k are shown in Fig. 4. The shapes of the reflectivity spectrum is similar to that the reflectance spectrum for 60°; however, the n and k

spectra are very different. It can be seen that the shapes of the n and k spectra near to the dips of the LO mode inverts with the shapes going the opposite way. As can be seen from the R spectrum at 75°, the shapes near the TO phonon mode remain undistorted although the shapes of the n and k spectra have been changed to the 'derivative-like' shapes. This is most probably due to the changes in n values which has been compensated by the changes of the k values or vice versa. At the vicinity of the LO phonon mode, it is found that both the n and k spectra form a peak (see the enlargement in the p-polarized spectra of the n and k at 75°); as a result, a peak was formed near the LO phonon mode, namely, as depicted in the polarized R spectrum at 75°.

(b) 6H-SiC substrate

For the 6H-SiC substrate, the effects of the incidence angle on both the shapes of the reststrahlen band and their optical phonon modes are less significant as compared to the GaN thin films. This is evident from Fig. 2 and Table I that there are no relative distortions or shift of both the reststrahlen bands shape and the optical phonon modes of 6H-SiC substrate were detected over the entire range of angles of incidence which is from 15° to 75°. Nevertheless, it is found that the shapes of the reststrahlen band around the TO phonon mode becomes more flatten and the dips due to the absorption from the LO phonon mode of the 6H-SiC disappear as the incidence angle increases. We believed these alterations are due to the changes of the n and the k as discussed previously. As in the case of GaN thin films, this effect does not affect the phonon modes of the 6H-SiC substrate. As evident from Table 1, the optical phonon modes of the 6H-SiC substrate are independent on the angle of the incidence beam.

V. CONCLUSIONS

In this work, we have measured the s- and p-polarized IR reflectivity spectra at various angle of incidence of wurtzite structure GaN epilayer on 6H-SiC. The reflection spectra are compared to the calculated spectra generated with a damped single harmonic oscillator model. The fitting of the theoretical to the experimental curves is good in all cases. As the angle of incidence was increased, it was found that the s-polarized spectra retain their overall shape; while the p-polarized spectra especially near to the LO phonon modes of the GaN thin films were distorted and a new feature was slowly formed. The distortion is believed to be due to the changes of the refractive index, n, and the extinction coefficient, k, near the LO mode. We have attributed this effect to the phase shift between the incidence and the reflected polarized IR beam. For the 6H-SiC substrate, the effects of the incidence angle on both their shapes of the reststrahlen band and their optical phonon modes are less significant as compared to the GaN thin films. In general, the optical phonon modes for GaN epilayer and 6H-SiC substrate are independent on the angle of the incidence beam.

ACKNOWLEDGMENT

The authors would like to acknowledge Universiti Sains Malaysia and IRPA RMK-8 Strategic Research grant for their financial support.

REFERENCES

1. S. Strite, M. E. Lin, and H. Morkoc, Thin Solid Films **231**, 197 (1993).
2. H. Morkoc, S. Strite, G. B. Gao, M. E. Lin, B. Sverdlov, and M. J. Burns, Appl. Phys. **76**, 1363 (1994).
3. D. Steigerwald, S. Rudaz, H. Liu, R. Scott Kern, W. Götz, and R. Fletcher, Journal of JOM **49**, 18 (1997).
4. P. Perlin, J. Camassel, W. Knap, T. Taliercio, J. C. Chervin, T. Suski, I. Grzegory, and S. Porowski, Appl. Phys. Lett. **67**, 2524 (1995).
5. P. Perlin, E. Litwin-Staszewska, B. Suchanek, W. Knap, J. Camassel, T. Suski, R. Piotrzkowski, I. Grzegory, S. Porowski, E. Kaminska, and J. C. Chervin, Appl. Phys. Lett. **68**, 1114 (1996).
6. M. F. MacMillan, R. P. Devaty, W. J. Choyke, M. Asif Khan, and J. Kuznia, J. Appl. Phys. **80**, 2372 (1996).
7. G. Yu, H. Ishikawa, M. Umeno, T. Egawa, J. Watanabe, T. Soga, and T. Jimbo, Appl. Phys. Lett. **73**, 1472 (1998).
8. A. Iller, W. Jantsch, J. Marks, B. Pastuszka, R. Diduszko, and J. Sadowski, Diamond and Related Materials **8**, 25 (1999).
9. Y. T. Hou, Z. C. Feng, S. J. Chua, M. F. Li, N. Akutsu and K. Matsumoto, Appl. Phys. Lett. **75**, 3117 (1999).
10. Z. F. Li, W. Lu, H. J. Ye, Z. H. Chen, X. Z. Yuan, H. F. Dou, and S. C. Shen, G. Li, and S. J. Chua, J. Appl. Phys. **86**, 2691 (1999).
11. E. Frayssinet, W. Knap, P. Prystawko, M. Leszczynski, I. Grzegory, T. Suski, B. Beaumont, and P. Gibart, J. Cryst. Growth **218**, 161 (2000).

12. Y. T. Hou, Z. C. Feng, J. Chen, X. Zhang, S. J. Chua, and J. Y. Lin, Solid State Commun. **115**, 45 (2000).

13. Z. C. Feng, T. R. Yang, and Y. T. Hou, Materials Science in Semiconductor Processing **4**, 571 (2001).

14. Z. C. Feng, X. Zhang, S. J. Chua, T. R. Yang, J. C. Deng, and G. Xu, Thin Solid Films **409**, 15 (2002).

15. X. Zhang, Y. T. Hou, Z. C. Feng, and J. L. Chen, J. Appl. Phys. **89**, 6165 (2001).

16. J. A. Bardwell, M. W. C. Dharma-Wardana, H. Tang, and J. B. Webb, J. Vac. Sci. Technol. A. **18**, 643 (2000).

17. D. D. Manchon, A. S. Barker, Jr., P. J. Dean, and R. B. Zetterstrom, Solid State Commun. **8**, 1227 (1970).

18. A. S. Barker and M. Ilegems, Phys. Rev. B 7, 743 (1973).

19. H. Sobotta, H. Neumann, R. Franzheld, and W. Seifert, Phys. Status Solidi B **174**, K57 (1992).

20. M. Hao, S. Mahanty, R. S. Qhalid Fareed, S. Tottori, K. Nishino, and S. Sakai, Appl. Phys. Lett. **74**, 2788 (1999).

21. C. Wetzel, E. E. Haller, H. Amano, and I Akasaki, Appl. Phys. Lett. **68**, 2547 (1996).

22. G. Mirjalili, T. Dumelow, T. J. Parker, S. F. Shayesteh, T. S. Cheng, C. T. Foxon, L. C. Jenkins, and D. E. Lacklinson, Infrared Phys. Technol. **37**, 389 (1996).

23. G. Mirjalili, T. J. Parker, S. F. Shayesteh, M. M. Bulbul, S. R. P. Smith, T. S. Cheng, and C. T. Foxon, Phys. Rev. B **57**, 4656 (1998).

24. G. Yu, N. L. Rowell, and D. J. Lockwood, J. Vac. Sci. Technol. A. **22**, 1110 (2004).

25. C. H. Yan, H. Yao, J. M. Van Hove, A. M. Wowchak, P. P. Chow, and J. M. Zavada, J. Appl. Phys. **88**, 3463 (2000).

26. A. Kasic, M. Schubert, S. Einfeldt, D. Hommel, T. E. Tiwald, Phys. Rev. B **62**, 7365 (2000).

27. M. Schubert, A. Kasic, T.E. Tiwald, J. Off, B. Kuhn, F. Scholz, MRS Internet J. Nitride Semicond. Res. **4**, 11 (1999).

28. J. Wang, X.Y. Li, J. Liu, Z. M. Huang, Semicond. Sci. Technol. **20**, 540 (2005).

29. S. S. Ng, L. S. Chuah, Z. Hassan, H. Abu Hassan, in: Che Mohamad Som Said, Mohd Rozi Ahmad (Eds.), Proceedings of Conference on Applied Sciences (CAS), University Publication Centre, Shah Alam, 2006, p. 255.

30. T. Dumelow, T. J. Parker, S. R. P. Smith, and D. R. Tilley, Surf. Sci. Rep. **37**, 151 (1993).

31. W. G. Spitzer, D. Kleinman, and D. Walsh, Phys. Rev. **113**, 127 (1959).

32. D. W. Berreman, Phys. Rev. **130**, 2193 (1963).

33. F. A. Jenkins and H. E. White, "Fundamentals of Optics, 4th ed," (McGraw-Hill, New York, 1976), Chp. 25.

34. V. Bougrov, M. Levinshtein, S. Rumyantsev, and A. Zubrilov, in *Properties of Advanced Semiconductor Materials*: *GaN, AlN, InN, BN, SiC, SiGe*, edited by M. E. Levinshtein, S. L. Rumyantsev, and M. S. Shur (John Wiley & Sons, Inc., New York, 2001), p. 3.

35. M. Claybourn, in *Handbook of Vibrational Spectroscopy, Vol. 2: Sampling Techniques*, edited by J. M. Chalmers, and P. R. Griffiths (John Wiley & Sons, Inc., New York, 2002), p. 969.

List of Tables Captions

TABLE I. Best-fit parameters for IR reflectance spectra of GaN epilayer grown on 6H-SiC substrate measured with s- and p-polarization radiation at different incidence angles.

List of Figures Captions

Fig. 1. Schematic diagram of the GaN/6H-SiC cross-section and the beam geometry of the polarization measurements.

Fig. 2. Polarized IR reflectance spectra for GaN/6H-SiC taken at different angles of incidence: (a) 15°; (b) 30°; (c) 45°; (d) 60°; (e) 75°. The dotted line represents the theoretical reflectance spectra.

Fig. 3. Real refractive index, n, and extinction coefficient, k, spectra for GaN/6H-SiC with s- and p-polarization at different angles of incidence: (a) 15°; (b) 30°; (c) 45°; (d) 60°; (e) 75°. The n and k spectra are obtained from the Kramer-Kronig dispersion relation.

Fig. 4. P-polarized IR reflectance spectrum for GaN/6H-SiC taken at Brewster angle of 66.5° of GaN epilayer. The dotted line and the dash line are the corresponding real refractive index, n, and extinction coefficient, k, respectively.

TABLE I. Best-fit parameters for IR reflectance spectra of GaN epilayer grown on 6H-SiC substrate measured with s- and p-polarization radiation at different incidence angles.

Polarization	Parameters	GaN (epilayer)					6H-SiC (substrate)				
		15°	30°	45°	60°	75°	15°	30°	45°	60°	75°
s-polarization	w_{LO} cm^{-1}	745.0 [a]	745.0 [a]	745.0 [a]	745.0 [a]	745.0 [a]	973.4 [a]	973.4 [a]	973.4 [a]	973.4 [a]	973.4 [a]
	w_{TO} cm^{-1}	557.5	557.5	557.5	557.5	557.5	796.0	796.0	796.0	796.0	796.0
	S	4.05	4.05	4.05	4.05	4.05	3.32	3.32	3.33	3.32	3.32
	ε_∞	5.14 [b]	5.14 [b]	5.14 [b]	5.14 [b]	5.14 [b]	6.7 [c]	6.7 [c]	6.7 [c]	6.7 [c]	6.7 [c]
	γ cm^{-1}	2.0	2.0	2.0	3.0	3.0	8.0	8.0	8.0	8.0	8.0
p-polarization	w_{LO} cm^{-1}	732.2	732.2	732.2	732.2	732.2	967.1	967.1	967.1	967.1	967.1
	w_{TO} cm^{-1}	557.5 [a]	557.5 [a]	557.5 [a]	557.5 [a]	557.5 [a]	794.0 [a]	794.0 [a]	794.0 [a]	794.0 [a]	794.0 [a]
	S	3.85	3.85	3.85	3.85	3.85	3.24	3.24	3.24	3.24	3.24
	ε_∞	5.31 [b]	5.31 [b]	5.31 [b]	5.31 [b]	5.31 [b]	6.7 [c]	6.7 [c]	6.7 [c]	6.7 [c]	6.7 [c]
	γ cm^{-1}	6.0	6.0	6.0	6.0	7.0	6.0	6.0	6.0	6.0	5.0

[a] Derived using Equation (5), i.e. $S = \varepsilon_\infty \left(\frac{w_{LO}^2 - w_{TO}^2}{w_{TO}^2} \right)$.

[b] Taken from Yu *et al.* (Reference 24).

[c] Taken from Spitzer *et al.* (Reference 31).

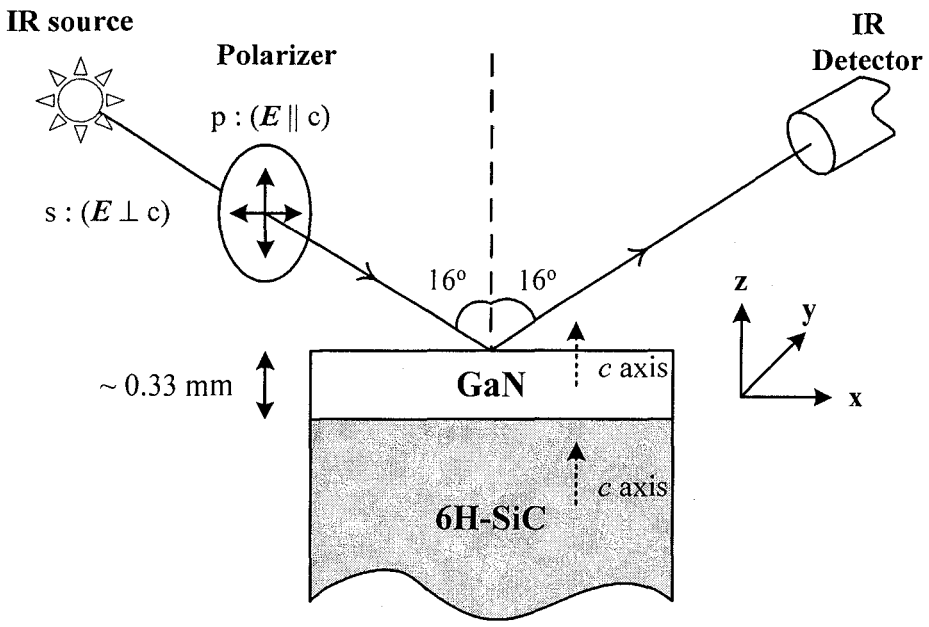

s : the electric field vector (*E*) is perpendicular to the plane of incidence

p : the electric field vector (*E*) is parallel to the plane of incidence

Fig. 1. Schematic diagram of the GaN/6H-SiC cross-section and the beam geometry of the polarization measurements.

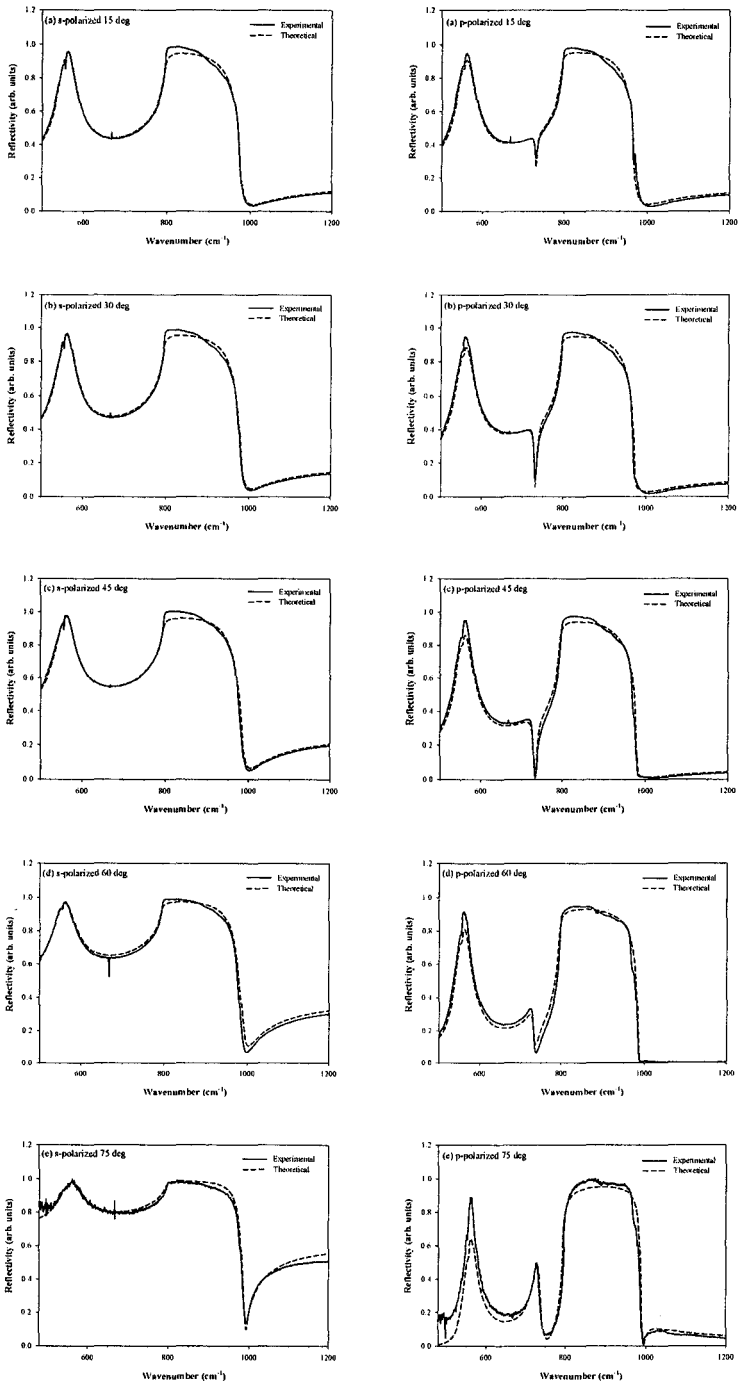

Fig. 2. Polarized IR reflectance spectra for GaN/6H-SiC taken at different angles of incidence: (a) 15°; (b) 30°; (c) 45°; (d) 60°; (e) 75°. The dotted line represents the theoretical reflectance spectra.

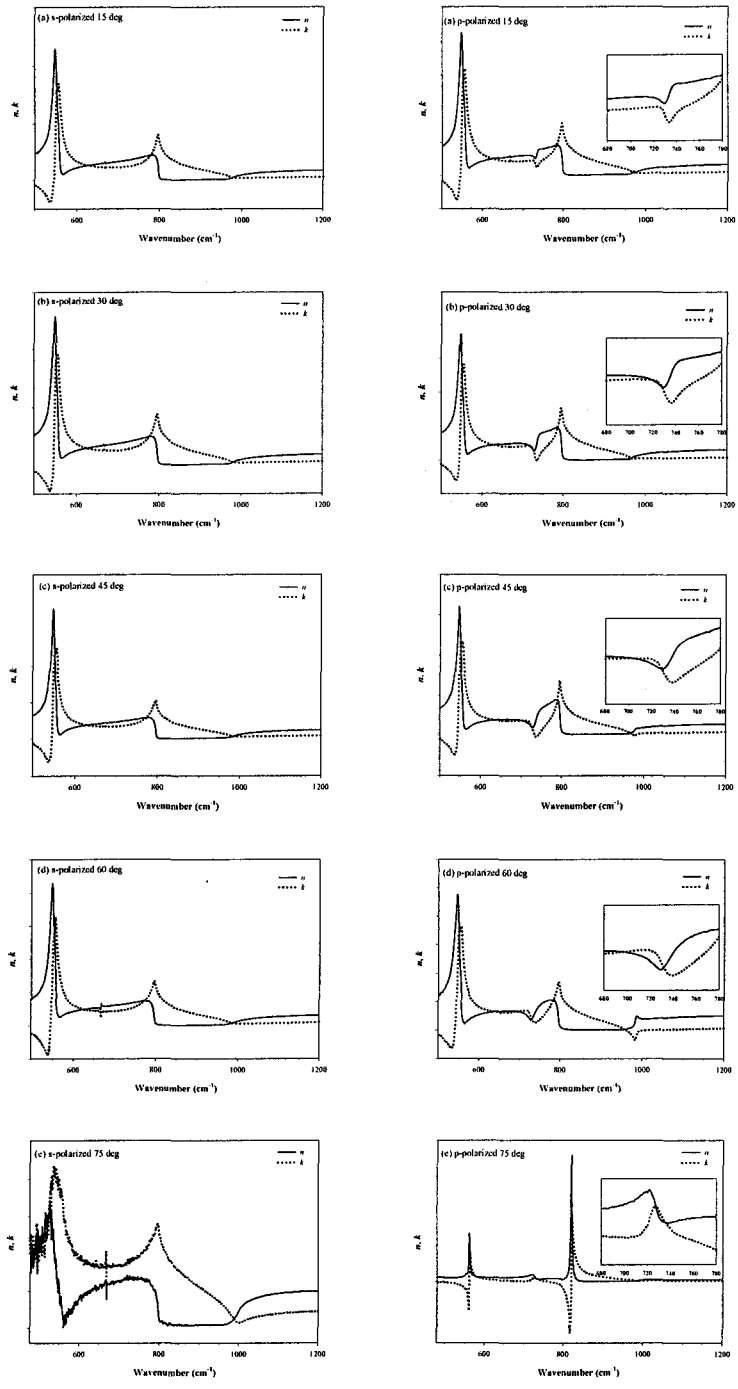

Fig. 3. Real refractive index, n, and extinction coefficient, k, spectra for GaN/6H-SiC with s- and p-polarization at different angles of incidence: (a) 15°; (b) 30°; (c) 45°; (d) 60°; (e) 75°. The n and k spectra are obtained from the Kramer-Kronig dispersion relation.

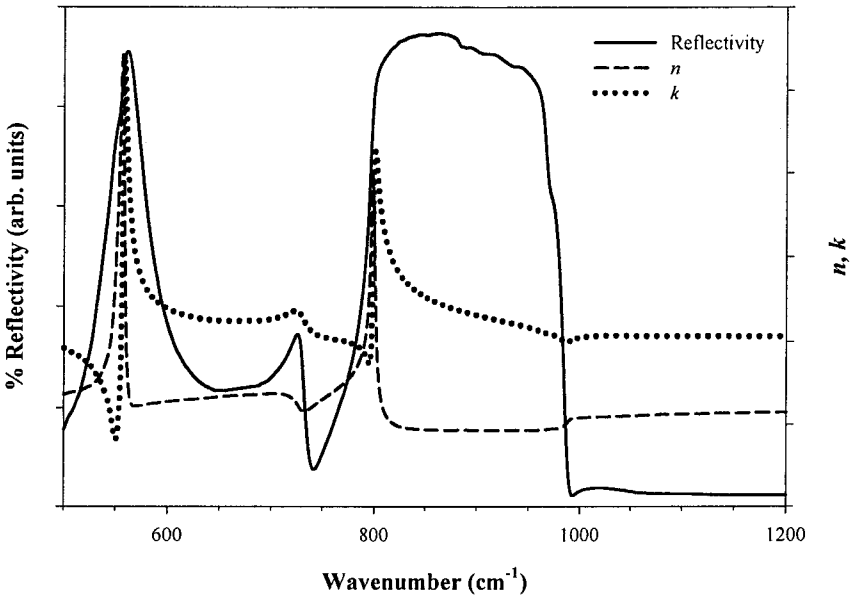

Fig. 4. P-polarized IR reflectance spectrum for GaN/6H-SiC taken at Brewster angle of 66.5° of GaN epilayer. The dash line and the dotted line are the corresponding real refractive index, n, and extinction coefficient, k, respectively.